Geochemical Perspectives Letters

Comparative ^{142}Nd and ^{182}W study of mid-ocean ridge basalts and the 4.5 Gyr evolution of the upper mantle

D. Peters, H. Rizo, J. O'Neil, C. Hamelin, S.B. Shirey

Supplementary Information

The Supplementary Information includes:

- Sample Description
- Methods
- Figures S-1 to S-4
- Data Tables S-1 to S-4
- Supplementary Information References

Sample Description

The mid-ocean ridge basalts studied here were sampled during the PACANTARCTIC2 cruise (2004-2005) along the Pacific Antarctic Ridge (PAR) between 53°S and 41°S (**Fig. S-1**). The goal of the PACANTARTIC2 cruise was to sample the ridge furthest away possible from any hotspot, in order to study the composition of the depleted upper mantle. The morphology (median values of the ridge axis bathymetry and ridge cross-section) of the ridge sampled during the PACANTARCTIC2 is consistent with a normal fast spreading ridge (*e.g.*, Briais *et al.*, 2009), which differs from a hotspot-ridge interaction setting. The closest hotspot-ridge interaction from the studied PAR area is the Foundation hotspot ~800 km north, and the 2nd closest is the Louisville hotspot ~1200 km south. The PAR is a fast-spreading context where along axis fluxes are limited, and thus hotspot contributions are negligible over such long distances. The lack of hotspot influence in the samples studied is further supported by geochemical studies (*e.g.*, Moreira *et al.*, 2008; Hamelin *et al.*, 2010, 2011; Labidi *et al.*, 2014; Bezard *et al.*, 2016). Trace element ratios, such as $(La/Sm)_N$ are within the domain of 'normal MORB' (Hamelin *et al.*, 2010). Geochemical compositions in Sr-Nd-Pb-Hf of these samples can be found in Hamelin *et al.* (2011) and plot close to the DMM end member. The range of radiogenic compositions in that study are attributed to the partial melting of a « marble-cake » mantle assemblage, unrelated to plume-ridge interactions. Additionally, helium isotopes of the Pacific-Antarctic Ridge between 41.5 and 52.5° S show a lack of hotspot influence along that section of the ridge (Moreira *et al.*, 2008).

Tungsten concentrations in the PAR MORBs studied here (n = 18) vary from 6.8 ng g^{-1} to 220 ng g^{-1} (**Data Table S-1**). The W concentrations are strongly coupled to other immobile and incompatible trace elements such as Nb and Th, and W/Th ratios are within the range of fresh MORB (**Fig. S-2**). This implies that W contained in the MORB samples studied is derived from their mantle sources (*e.g.*, König *et al.*, 2011) and free from secondary W overprinting.

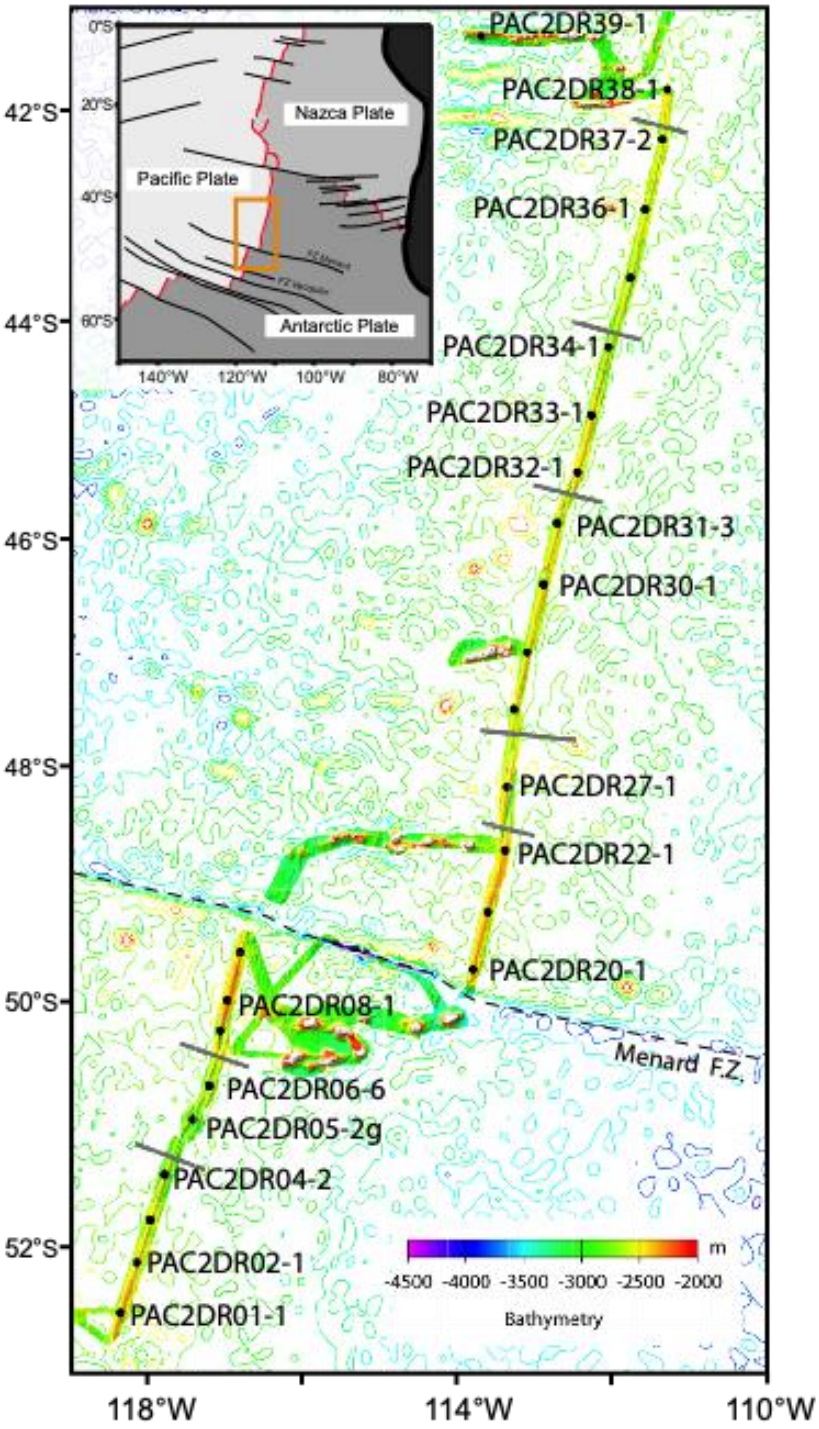

Figure S-1 Map of the Pacific-Antarctic Ridge. Black dots are dredged samples during the PACANTARCTIC2 cruise. Grey lines are overlapping spreading centres (OSC) bordering second order segmentation of the ridge axis.

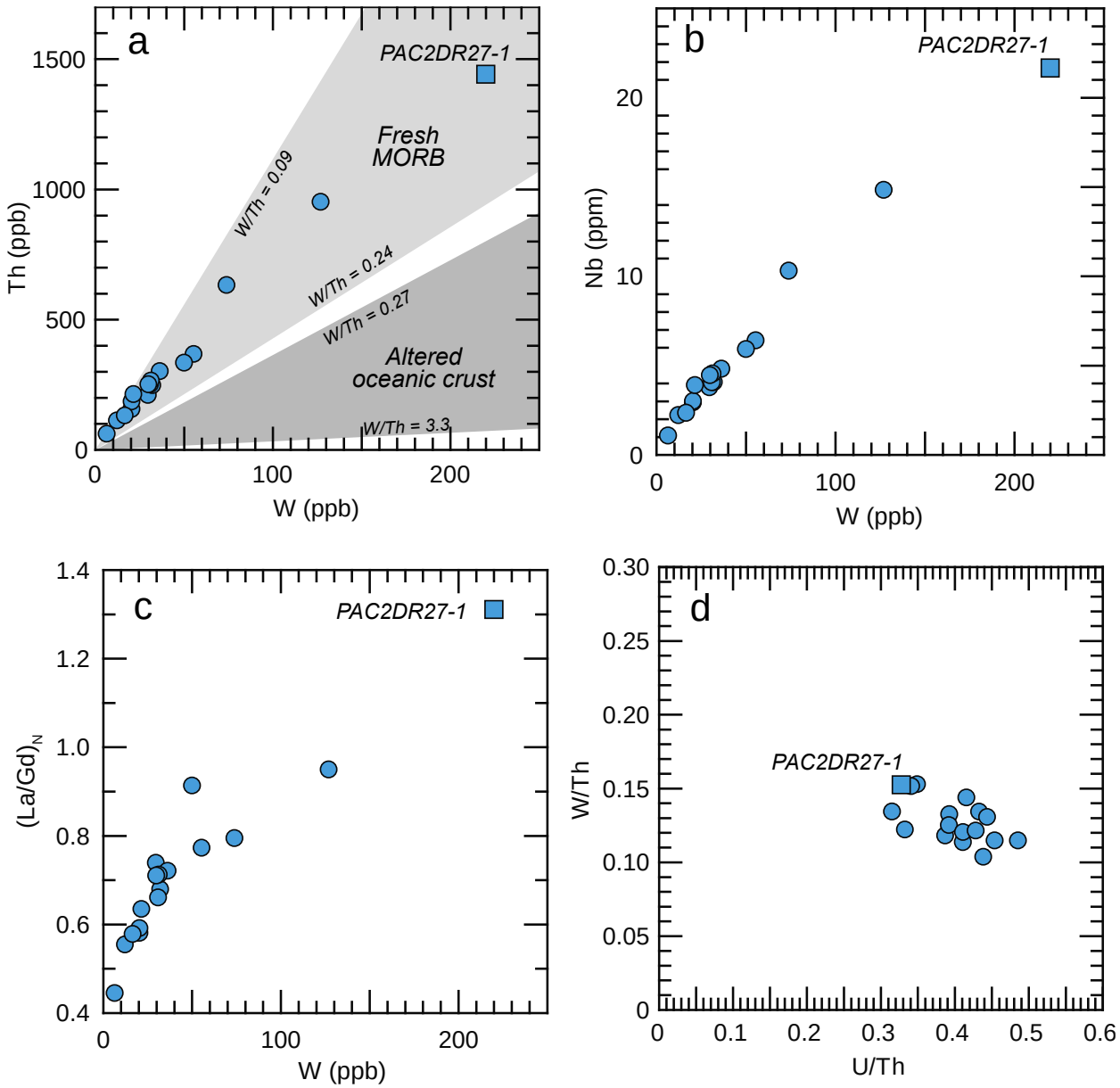

Figure S-2 Tungsten vs. other highly incompatible trace element concentrations and the normalized La/Gd ratio of the Pacific-Atlantic ridge basalts. Tungsten concentrations from this study, other trace element concentrations from Hamelin *et al.* (2010), Labidi *et al.* (2014) and Yierpan *et al.* (2019). Fresh MORB W/Th ranges from König *et al.* (2011), altered oceanic crust W/Th ranges from Reifenröther *et al.* (2021).

Methods

Tungsten concentration analysis

Tungsten concentrations (**Data Table S-1**) were determined by isotope dilution using a ^{186}W spike. Approximately 0.1 g of sample powder was dissolved in a mixture of 4 mL 29 M HF and 1 mL 15 M HNO_3,

followed by repeated dissolutions in 1 mL 6N HCl. Samples were spiked at the onset of digestion to insure sample-spike equilibration. Tungsten was isolated using ion chromatography techniques similar to the ones described in Nagai and Yokoyama (2014). Isotope ratio measurements were carried out on a ThermoScientific Neptune MC-ICPMS of the Isotope Geochemistry and Geochronology Research Centre (IGGRC) of Carleton University (Ottawa, Canada). Measurements were performed on 1.5 ppb W 0.5 M HNO_3 + 0.05 HF solutions. Two standard deviation measurement precisions are largely 2-4 %, propagated 2 standard deviations are estimated better than 10 % in most cases (largely by uncertainty of the spike concentration). Monitoring the measurement accuracy of isotope dilution concentration analysis with the USGS basalt standards BHVO-2 and BCR-2 yielded 193 ± 18 ng g^{-1} and 436 ± 47 ng g^{-1}, respectively, which are similar within errors of previously reported concentrations (*e.g.*, Jochum *et al.*, 2016; Kurzweil *et al.*, 2018). Total chemistry blanks were 260 pg, representing 1-2 % of the W analysed in samples.

Tungsten isotope analysis

High precision W isotope compositions (**Data Table S-2**) were also obtained at the IGGRC of Carleton University. Sample masses between 3.4 g and 24.5 g were dissolved and W was separated following similar methods described in Touboul and Walker (2012) and Breton and Quitté (2014). Tungsten separation for isotope analysis was performed using a first 20 mL AG50W-X8 resin (200-400 mesh) column to remove matrix elements, and a second 10 mL AG1-X8 resin (200–400 mesh) column to separate W from other high field strength elements (HFSE). Purified W solutions were passed through an additional AG1-X8 resin (200–400 mesh) micro-column (0.3 mL) mainly to remove Ti traces that could reduce the ionization efficiency of W. Tungsten yields were 50-70 %, procedural blanks ranged between 0.4 to 3.0 ng, respectively, for ~ 440 to 530 ng of W separates representing less than 1 % of the total W.

Tungsten isotope ratios were measured on a ThermoScientific Triton TIMS, using the setup and protocols described in Archer *et al.* (2017) and Rizo *et al.* (2019). Results were interference-corrected using the oxygen isotope compositional relations from Archer *et al.* (2017) and mass bias-corrected by internal normalisation to $^{186}W/^{184}W = 0.92767$ (Völkening *et al.*, 1991) (normalisation to $^{186}W/^{183}W = 1.985936$ was also performed and results shown in **Data Table S-2**). The $^{182}W/^{184}W$ and $^{183}W/^{184}W$ ratios are reported as μ notations, which are deviations in parts per million (ppm) from the isotope composition of the Alfa Aesar W standard. This standard yielded $^{182}W/^{184}W = 0.864888 \pm 0.000003$ (2 s.d.; n = 6), and $^{183}W/^{184}W = 0.467149 \pm 0.000001$ (2 s.d.; n = 7). Two additional measurements of the NIST standard 3163 yielded mean $\mu^{182}W = 2.4 \pm 6.0$ (2 s.d.) and $\mu^{183}W = -1.4 \pm 2.9$ (2 s.d.). No residual mass-dependent fractionation is observed in the dataset (**Fig. S-3**). The $\mu^{182}W$ errors of means are ± 2σ standard deviations (2 s.d.) of the sample populations, or 2σ standard errors (2 s.e.) of the individual measurements.

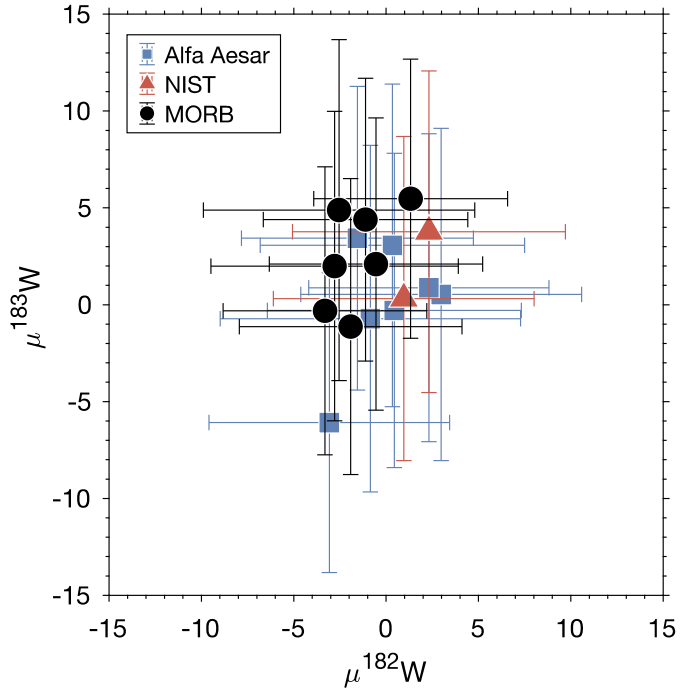

Figure S-3 $\mu^{183}W$ vs $\mu^{182}W$ of the MORB samples of this study, as well as of the Alfa Aesar W standard and the W isotope standard reference material 3163 from the National the Institute of Standards and Technology (NIST). Both $\mu^{183}W$ vs $\mu^{182}W$ shown are mass bias-corrected using $^{186}W/^{184}W$.

Neodymium isotope analysis

Fourteen MORB samples have been analysed for high-precision Nd isotopic compositions (**Data Table S-3**). Chemical separation and purification of Nd were performed at the Advanced Research Complex of University of Ottawa, Canada, following the protocols of Garçon *et al.* (2018) and Li *et al.* (2015), and only the main steps are summarized here. The light-REE were separated from the whole-rock matrix using 200-400 mesh AG50W-X8 cation-exchange resin. The dried light-REE fractions were dissolved in HNO_3 with $NaBrO_3$ to oxidize Ce to its +4 form and remove it from other light-REE+3 using columns filled with 100-150 µm Eichrom LnSpec resin. The Na and Br added during the Ce-removal procedure were then removed using AG50W-X8 cation-exchange resin. The Nd was finally purified from Sm and any remaining Ce using thin columns filled with 20-50 µm Eichrom LnSpec resin. Total chemistry Nd yields were ≥ 90 %, the total procedural Nd blank was 16 pg.

High-precision Nd isotope abundance ratio measurements were performed on a ThermoScientific Triton TIMS at the Isotope Geochemistry and Geochronology Research Centre of Carleton University (Ottawa, Canada). Samples were loaded onto zone-refined 99.999 % Re filaments and Nd isotopes were measured on double filaments and using a 2-step dynamic routine that provided static measurements of all Nd abundance isotope ratios and dynamic measurements of the $^{142}Nd/^{144}Nd$ ratio. The mass/charge ratios 140^+ and 147^+ were monitored for Ce and Sm mass interference corrections. Each run consisted of 600 to 1200 ratios measured in blocks of 25 cycles, with an integration time of 8.39 seconds per step and a background measurement of 30s between each block. Data were corrected for instrumental mass fractionation using the exponential law to $^{146}Nd/^{144}Nd = 0.7219$. Samples were measured at the same time as the JNdi-1 Nd standard, and in two

analytical sessions (Session 1 and Session 2; **Data Table S-3**). For Session 1, repeated measurement of the JNdi-1 standard yielded an average $^{142}Nd/^{144}Nd = 1.141835 \pm 0.000004$ (2 s.d., n = 14), corresponding to a repeatability of 3.8 ppm. For Session 2, the JNdi-1 yielded an average $^{142}Nd/^{144}Nd = 1.141836 \pm 0.000004$ (2 s.d., n = 6), corresponding to a repeatability of 3.3 ppm. The average $^{143}Nd/^{144}Nd$ ratio for the JNdi-1 standard for both sessions was 0.512107 ± 0.000003 (2 s.d.), and within error of the value of Tanaka *et al.* (2000) of 0.512115 ± 0.000007. The $\mu^{142}Nd$ errors of means are ± 2σ standards deviations (2 s.d.) of the sample populations or 2σ standard errors (2 s.e.) of the individual measurements.

The $\mu^{142}Nd$ obtained for the PAR MORB samples do not correlate with their $\mu^{182}W$ (**Fig. S-4**).

A database for all available $\mu^{142}Nd$ for MORB, OIB and mantle peridotites is provided in the **Data Table S-4**.

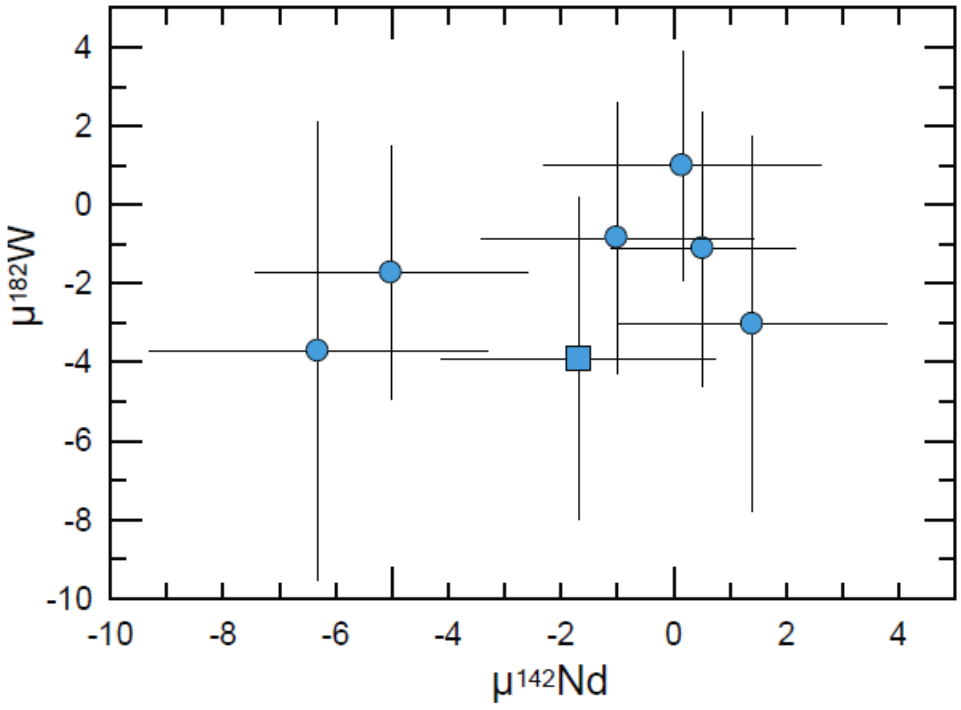

Figure S-4 $\mu^{182}W$ *vs.* $\mu^{142}Nd$ of the PAR MORB samples of this study. Errors shown are ± 2 s.e. Square symbol for sample PAC2DR27-1 (T-MORB).

Supplementary Information Data Tables

Data Tables S-1 to S-4 (Excel) can be downloaded from the online version of this article at https://doi.org/10.7185/geochemlet.2412.

Data Table S-1 Tungsten abundances for the PAR MORB samples of this study, and the USGS rock reference materials BHVO-2 and BCR-2.

Data Table S-2 Detailed high-precision W isotope measurements for the PAR MORB samples of this study. Tungsten isotope ratios normalised to $^{186}W/^{184}W$ (spreadsheet 1), or $^{186}W/^{183}W$ (spreadsheet 2).

Data Table S-3 Detailed high-precision Nd isotope measurements for the PAR MORB samples of this study.

Data Table S-4 Compilation of published $\mu^{142}Nd$ and $\mu^{182}W$ for MORB, OIB and mantle peridotites.

Supplementary Information References

Andreasen, R., Sharma, M., Subbarao, K.V., Viladkar, S.G. (2008) Where on Earth is the enriched Hadean reservoir?. *Earth and Planetary Science Letters* 266, 14-28. https://doi.org/10.1016/j.epsl.2007.10.009

Archer, G. J., Mundl, A., Walker, R.J., Worsham, E.A., Bermingham, K.R. (2017) High-precision analysis of $^{182}W/^{184}W$ and $^{183}W/^{184}W$ by negative thermal ionization mass spectrometry: Per-integration oxide corrections using measured $^{18}O/^{16}O$. *International Journal of Mass Spectrometry* 414, 80–86. https://doi.org/10.1016/j.ijms.2017.01.002

Bezard, R., Fischer-Gödde, M., Hamelin, C., Brennecka, G.A., Kleine, T. (2016) The effects of magmatic processes and crustal recycling on the molybdenum stable isotopic composition of Mid-Ocean Ridge Basalts. *Earth and Planetary Science Letters* 453, 171-181. https://doi.org/10.1016/j.epsl.2016.07.056

Boyet, M., Carlson, R.W. (2006) A new geochemical model for the Earth's mantle inferred from 146Sm–142Nd systematics. *Earth and Planetary Science Letters* 250, 254-268. https://doi.org/10.1016/j.epsl.2006.07.046

Breton, T., Quitté, G. (2014) High-precision measurements of tungsten stable isotopes and application to Earth sciences. *Journal of Analytical Atomic Spectrometry* 29, 2284-2293.https://doi.org/10.1039/C4JA00184

Briais, A., Ondreas, H., Klingelhoefer, F., Dosso, L., Hamelin, C., Guillou, H. (2009) Origin of volcanism on the flanks of the Pacific - Antarctic ridge between 41 ° 30' S and 52° S. *Geochemistry, Geophysics, Geosystems* 10, 9. https://doi.org/10.1029/2008GC002350

Caro, G., Bourdon, B., Birck, J.L., Moorbath, S. (2006) High-precision $^{142}Nd/^{144}Nd$ measurements in terrestrial rocks: constraints on the early differentiation of the Earth's mantle. *Geochimica et Cosmochimica Acta* 70, 164-191. https://doi.org/10.1016/j.gca.2005.08.015

Cipriani, A., Bonatti, E., Carlson, R.W. (2011) Nonchondritic 142Nd in suboceanic mantle peridotites. *Geochemistry, Geophysics, Geosystems* 12. https://doi.org/10.1029/2010GC003415

Garçon, M., Boyet, M., Carlson, R.W., Horan, M.F., Auclair, D., Mock, T.D. (2018) Factors influencing the precision and accuracy of Nd isotope measurements by thermal ionization mass spectrometry. *Chemical Geology* 476, 493-514. https://doi.org/10.1016/j.chemgeo.2017.12.003

Hamelin, C., Dosso, L., Hanan, B., Barrat, J.A., Ondréas, H. (2010) Sr - Nd - Hf isotopes along the Pacific Antarctic Ridge from 41 to 53° S. *Geophysical Research Letters* 37, 10.

Hamelin, C., Dosso, L., Hanan, B.B., Moreira, M., Kositsky, A.P., Thomas, M.Y. (2011) Geochemical portray of the Pacific Ridge: New isotopic data and statistical techniques. *Earth and Planetary Science Letters* 302, 154-162. https://doi.org/10.1016/j.epsl.2010.12.007

Horan, M.F., Carlson, R.W., Walker, R.J., Jackson, M., Garçon, M., Norman, M. (2018) Tracking Hadean processes in modern basalts with 142-Neodymium. *Earth and Planetary Science Letters*, 484, 184-191.https://doi.org/10.1016/j.epsl.2017.12.017

Hyung, E., Jacobsen, S.B. (2020) The 142Nd/144Nd variations in mantle-derived rocks provide constraints on the stirring rate of the mantle from the Hadean to the present. *Proceedings of the National Academy of Sciences*, 117, 14738-14744. https://doi.org/10.1073/pnas.2006950117

Jackson, M.G., Carlson, R.W. (2012) Homogeneous superchondritic $^{142}Nd/^{144}Nd$ in the mid - ocean ridge basalt and ocean island basalt mantle. *Geochemistry, Geophysics, Geosystems* 13. https://doi.org/10.1029/2012GC004114

Jackson, M.G., Blichert-Toft, J., Halldórsson, S.A., Mundl-Petermeier, A., Bizimis, M., Kurz, M.D., Price, A.A., Harðardóttir, S., Willhite, L.N., Breddam, K., Becker, T.W., Fischer, R.A. (2020) Ancient helium and tungsten isotopic signatures preserved in mantle domains least modified by crustal recycling. *Proceedings of the National Academy of Sciences*, 117, 30993-31001. https://doi.org/10.1073/pnas.2009663117

Jochum, K.P., Weis, U., Schwager, B., Stoll, B., Wilson, S.A., Haug, G.H., Andreae, M.O., Enzweiler, J. (2016) Reference values following ISO guidelines for frequently requested rock reference materials. *Geostandards and Geoanalytical Research* 40, 333-350. https://doi.org/10.1111/j.1751-908X.2015.00392.x

König, S., Münker, C., Hohl, S., Paulick, H., Barth, A.R., Lagos, M., Pfänder, J., Büchl, A. (2011) The Earth's tungsten budget during mantle melting and crust formation. *Geochimica et Cosmochimica Acta* 75, 2119-2136. https://doi.org/10.1016/j.gca.2011.01.031

Kruijer, T.S., Kleine, T. (2018) No 182W excess in the Ontong Java Plateau source. *Chemical Geology* 485, 24-31. https://doi.org/10.1016/j.chemgeo.2018.03.024

Kurzweil, F., Münker, C., Tusch, J., Schoenberg, R. (2018) Accurate stable tungsten isotope measurements of natural samples using a 180W-183W double-spike. *Chemical Geology* 476, 407-417. https://doi.org/10.1016/j.chemgeo.2017.11.037

Labidi, J., Cartigny, P., Hamelin, C., Moreira, M., Dosso, L. (2014) Sulfur isotope budget (32S, 33S, 34S and 36S) in Pacific–Antarctic ridge basalts: A record of mantle source heterogeneity and hydrothermal sulfide assimilation. *Geochimica et Cosmochimica Acta* 133, 47-67. https://doi.org/10.1016/j.gca.2014.02.023

Li, C.F., Wang, X.C., Li, Y.L., Chu, Z.Y., Guo, J.H., Li, X.H. (2015) Ce–Nd separation by solid-phase micro-extraction and its application to high-precision $^{142}Nd/^{144}Nd$ measurements using TIMS in geological materials. *Journal of Analytical Atomic Spectrometry* 30, 895-902. https://doi.org/10.1039/C4JA00328D

Mei, Q.F., Yang, J.H., Yang, Y.H. (2018) An improved extraction chromatographic purification of tungsten from a silicate matrix for high precision isotopic measurements using MC-ICPMS. *Journal of Analytical Atomic Spectrometry* 33, 569-577. https://doi.org/10.1039/C8JA00024G

Moreira, M.A., Dosso, L., Ondréas, H. (2008) Helium isotopes on the Pacific - Antarctic ridge (52.5°–41.5°S). *Geophysical Research Letters* 35, 10. https://doi.org/10.1029/2008GL033286

Mundl, A., Touboul, M., Jackson, M.G., Day, J.M.D., Kurz, M.D., Lekic, V., Helz, R.T., Walker, R.J. (2017) Tungsten-182 heterogeneity in modern ocean island basalts. *Science* 356, 66–69. https://doi.org/10.1126/science.aal4179

Mundl-Petermeier, A., Walker, R.J., Jackson, M.G., Blichert-Toft, J., Kurz, M.D., Halldórsson, S.A. (2019) Temporal evolution of primordial tungsten-182 and $^{3}He/^{4}He$ signatures in the Iceland mantle plume. *Chemical Geology* 525, 245–259. https://doi.org/10.1016/j.chemgeo.2019.07.026

Mundl-Petermeier, A., Walker, R.J., Fischer, R.A., Lekic, V., Jackson, M G., Kurz, M D. (2020) Anomalous 182W in high 3He/4He ocean island basalts: Fingerprints of Earth's core? *Geochimica et Cosmochimica Acta* 271, 194–211. https://doi.org/10.1016/j.gca.2019.12.020

Murphy, D.T., Brandon, A.D., Debaille, V., Burgess, R., Ballentine, C. (2010) In search of a hidden long-term isolated sub-chondritic $^{142}Nd/^{144}Nd$ reservoir in the deep mantle: Implications for the Nd isotope systematics of the Earth. *Geochimica et Cosmochimica Acta* 74, 738-750. https://doi.org/10.1016/j.gca.2009.10.005

Nagai, Y., Yokoyama, T. (2014) Chemical separation of Mo and W from terrestrial and extraterrestrial samples via anion exchange chromatography. *Analytical Chemistry* 86, 4856–48630. https://doi.org/10.1021/ac404223t

Peters, B.J., Mundl-Petermeier, A., Carlson, R.W., Walker, R.J., Day, J.M.D. (2021) Combined Lithophile-Siderophile Isotopic Constraints on Hadean Processes Preserved in Ocean Island Basalt Sources. *Geochemistry, Geophysics, Geosystems* 22, 1–20. https://doi.org/10.1029/2020GC009479

Peters, B.J., Carlson, R.W., Day, J.M. Horan, M.F. (2018) Hadean silicate differentiation preserved by anomalous 142Nd/144Nd ratios in the Réunion hotspot source. *Nature* 555, 89-93. https://doi.org/10.1038/nature25754

Reifenröther, R., Münker, C., Scheibner, B. (2021) Evidence for tungsten mobility during oceanic crust alteration. *Chemical Geology* 584, 120504. https://doi.org/10.1016/j.chemgeo.2021.120504

Rizo, H., Walker, R.J., Carlson, R.W., Horan, M.F., Mukhopadhyay, S., Manthos, V., Francis, D., Jackson, M.G. (2016) Preservation of Earth-forming events in the tungsten isotopic composition of modern flood basalts. *Science* 352, 809-812. https://doi.org/10.1126/science.aad8563

Rizo, H., Andrault, D., Bennett, N. R., Humayun, M., Brandon, A., Vlastélic, I., Moine, B., Poirier, A., Bouhifd, M.A., Murphy, D.

T. (2019) ^{182}W evidence for core-mantle interaction in the source of mantle plumes. *Geochemical Perspectives Letters* 11, 6-11.https://doi.org/10.7185/geochemlet.1917

Tanaka, T., Togashi, S., Kamioka, H., Amakawa, H., Kagami, H., Hamamoto, T., Yuhara, M., Orihashi, Y., Yoneda, S., Shimizu, H., Kunimaru, T. (2000) JNdi-1: a neodymium isotopic reference in consistency with LaJolla neodymium. *Chemical Geology* 168, 279-281. https://doi.org/10.1016/S0009-2541(00)00198-4

Touboul, M., Walker, R.J. (2012) High precision tungsten isotope measurement by thermal ionization mass spectrometry. *International Journal of Mass Spectrometry* 309, 109-117. https://doi.org/10.1016/j.ijms.2011.08.033

Völkening, J., Köppe, M., Heumann, K.G. (1991) Tungsten isotope ratio determinations by negative thermal ionization mass spectrometry. *International Journal of Mass Spectrometry and Ion Processes* 107, 361-368. https://doi.org/10.1016/0168-1176(91)80070-4

Yierpan, A., König, S., Labidi, J., Schoenberg, R. (2019) Selenium isotope and S-Se-Te elemental systematics along the Pacific-Antarctic ridge: Role of mantle processes. *Geochimica et Cosmochimica Acta* 249, 199-224. https://doi.org/10.1016/j.gca.2019.01.028